Journal of Thermal Analysis, Vol. 40 (1993) 1017-1024

APPLICATION OF TIME AND TEMPERATURE RESOLVED X-RAY DIFFRACTION (TRXRD) TO THERMAL ANALYSIS

W. Engel, N. Eisenreich, M. Alonso and V. Kolarik

FRAUNHOFERINSTITUT FÜR CHEMISCHE TECHNOLOGIE
JOSEPH VON FRAUNHOFER-Str. 7, D–7507 BERGHAUSEN, FRG

The application of TRXRD for thermal analysis is demonstrated using examples of phase transitions, solid-state reactions and high-temperature corrosion. The measuring system produces a series of diffraction patterns, which are evaluated by a difference procedure that a reduces the data to curves comparable to DSC and TG curves and thus suited to kinetic evaluation.

Keywords: ammonium nitrate, application of TRXRD, high-temperature corrosion, kinetics, phase transitions, potassium nitrate, solid-state reactions

Introduction

TRXRD was first accomplished using photographic techniques [1–3], until semiconductor detectors allowed shorter measuring times with X-ray diffractometers and digital recording [4]. The technique has great potential, especially since the availability of synchrotron radiation has cut measuring times substantially.

This paper describes the application of TRXRD to thermal analysis of crystalline systems, where techniques such as DSC and TG cannot provide sufficient information. Such examples are in phase transitions where the identification of phases is required to avoid ambiguity or when sensitivity is a problem in DSC measurements of slow solid-state reactions.

In the case of ammonium nitrate, identification of the phases in transition is required, as several phases may occur within a relatively short temperature range [5, 6]. DSC peaks cannot reliably determine which phases change into each other.

The reaction of $Cu(OH)_2 \cdot CuCO_3$ with NH_4NO_3 demonstrates the potential of the technique for investigation of solid-state reactions, when isothermal experiments are carried out.

John Wiley & Sons, Limited, Chichester
Akadémiai Kiadó, Budapest

The high-temperature corrosion of steel represents an example of a complex solid-state/gas-phase reaction, where up to three layers or Fe_2O_3, Fe_3O_4 and FeO may grow on the metal surface. To avoid ambiguities the phases must be identified and their growth must be followed *in situ*. Non-isothermal measurements are presented to demonstrate the application of non-isothermal kinetics.

Measurements

Measurements were performed with a system described elsewhere [7]. This consists of an X-ray diffractometer combined with a low- or high-temperature device. With a fast position-sensitive proportional counter, more than 200 angle-dispersive diffraction patterns per day can be measured while the samples are heated and cooled linearly or stepwise with freely selectable temperature programs. In this way the samples can be monitored with respect to temperature or time.

The phase transitions and reactions of ammonium nitrate were measured with chromium radiation and a low-temperature device, whereas the steel corrosion was investigated using copper radiation and a high-temperature device. Samples of ARMCO-iron were heated in air from 25°–550°C in steps of 20°C at an average heating rate of 4.7deg·min^{-1}.

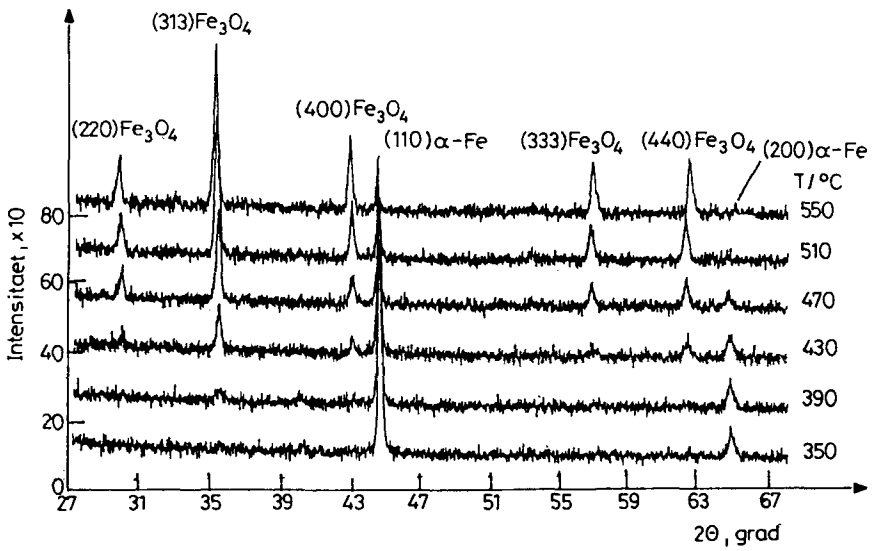

Fig. 1 Selected diffraction patterns of a high-temperature corrosion series

As an example of a measured series, Fig. 1 shows selected patterns from high-temperature corrosion measurements.

Evaluation

The evaluation can be performed by fitting diffraction peaks (peak position and intensity). The peak positions are used for calculations of lattice spacings and unit cell parameters. Plotting these values against time or temperature provides information on thermal expansion or change in peak intensity, i.e. concentration of a phase with time or temperature.

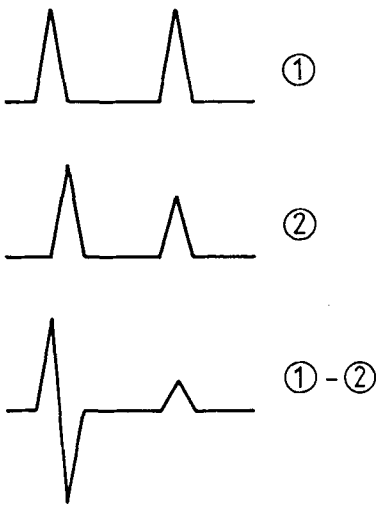

Fig. 2 Schematic explanation of difference formation between diffraction patterns

A different procedure, emphasized here and described elsewhere [8], utilizes difference diagrams of all adjacent patterns in the series (Fig. 2). Plotting the absolute sums of the difference diagrams against temperature yields a DSC-like curve,

$$DY(T_i) = \sum_{j=1}^{N} | X_j(T_i) - X_j(T_{i-1}) | ; \qquad i = 2,.....M$$

where N number of channels, j index channel no., X_j content j-th channel of i-th pattern, T_i independent variable, e.g. temperature.

If the difference diagrams are constructed using a constant reference pattern, e.g. the first one, then a TG-like curve is obtained.

$$Y(T_i) = \sum_{j=1}^{N} | X_j(T_1) - X_j(T_i) | ; \qquad i = 2,.....M$$

Figure 3 gives an example of a difference curve obtained with a mixture of ammonium nitrate and ZnO. The first step of the Y-curve and the first peak of the DY-curve shows the phase transition of ammonium nitrate at 55°C. The second step/peak indicates the solid-state reaction.

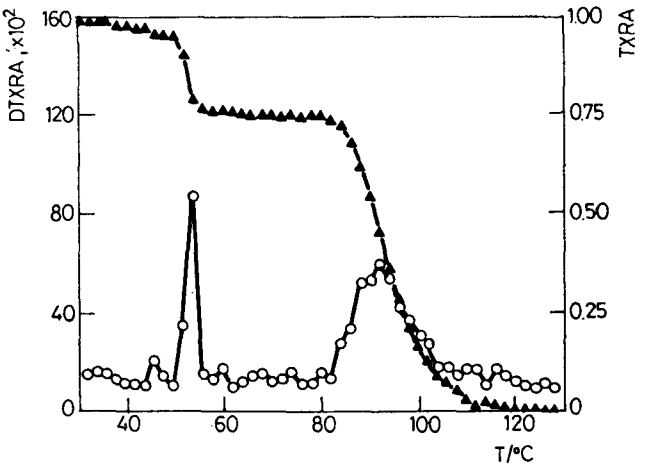

Fig. 3 Difference curves $DY(T)$ and $Y(T)$ obtained from measurements of a mixture of NH_4NO_3/ZnO

Phase transitions of ammonium nitrate doped with potassium nitrate

Ammonium nitrate was melted with 1, 3 and 5 mol% of KNO_3. The addition of KNO_3 extends the stability range of phase III [9–11]. The samples were cycled between –70° and 150°C. TRXRD was used because the DSC peaks listed in Table 1 could not be unambiguously attributed to the transitions of well-defined phases on cooling. The TRXRD series were evaluated with the difference procedure, and the phases participating in the transitions were identified from their diagnostic sets of peaks in the original patterns.

Ammonium nitrate plus 1 mol% KNO_3 changes on cooling at 45°C from phase II into phase IV, skipping phase III. With 3 mol%, phase II changes into phase III at about the same temperature, a difference that could not be detected with DSC (for more details see [7]).

Table 1 DSC results for NH_4NO_3/KNO_3

mol%	Phase transition temperatures /°C									
KNO_3	20 →150			150 → –60				–60 →150		
1	40	100	128	125	46	–32	–8	49	106	129
3		103	128	125	44	–30	–2	35	108	133
5		111	129	125	42	–28	+1	23	114	143

Solid-state reaction NH_4NO_3 + $Cu(OH)_2 \cdot CuCO_3$

This solid-state reaction is used to demonstrate the use of TRXRD for determining reaction kinetics from isothermal measurements. As with NH_4NO_3 + CuO [8], the reaction yields the diammine complex $[(NH_3)_2Cu](NO_3)_2$, which is of interest because it influences the phase transitions of ammonium nitrate.

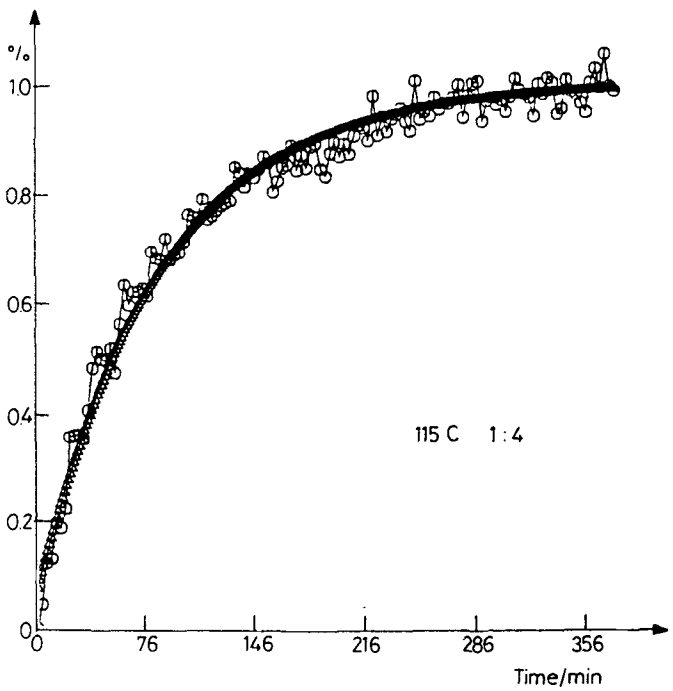

Fig. 4 Difference curve of an isothermal series measured with a mixture of $NH_4NO_3/Cu(OH)_2 \cdot CuCO_3$, molar ratio 4:1

Isothermal measurements were carried out at molar ratios of 4:1 and 8:1 at 110°, 115°, 120°, 125° and 130°C with time intervals of 3 min between the meas-

urements. The series were evaluated using the difference procedure. The resulting curves were normalized to 1 for complete reaction and fitted with

$$x(t) = 1 - e^{-kt}$$

assuming a first-order reaction. A fitted difference curve is shown in Fig. 4 and the fitted reaction constants are listed in Table 2.

Table 2 Reaction constants of the reaction of NH_4NO_3 with $Cu(OH)_2 \cdot CuCO_3$

Mol. ratio	4:1	8:1
Temp. / °C	$k \cdot 10^{-2}$	$k \cdot 10^{-2}$
110	0.61	1.92
115	1.25	2.12
120	1.85	3.03
125	2.33	7.38
130	2.82	7.73

From an Arrhenius plot slightly different values were obtained for the activation energies of the different molar ratios of the starting materials. The differences are higher for the pre-exponential factor, which reflects the easier transport of the reacting species with an excess of ammonium nitrate.

Table 3 Kinetic data obtained with the solid-state reaction $NH_4NO_3/Cu(OH)_2 \cdot CuCO_3$

Ratio	Activation energy / kJ	Pre-exponential factor, log Z
4:1	40	12.3
8:1	44	10.7

High-temperature corrosion of iron

The oxidation of iron in air was chosen to demonstrate the calculation of kinetic data from a non-isothermal series [12]. Figure 1 shows selected patterns of a series with stepwise heating.

After the experiment the end thickness of the oxide layer was determined microscopically. The difference curve $Y(T)$ was normalized to 1 and multiplied by the end thickness. The resulting curve $x(T)$ in Fig. 5 representing the growth of the oxide layer was used for kinetic evaluation.

The curve fitted to the difference curve is based on the parabolic time law for diffusion reactions (1):

$$dx/dt = k/x \qquad (1)$$

$$\alpha = dT/dt \tag{2}$$

$$k = z.e^{-E/RT} \tag{3}$$

After introducing the heating rate α (2) and the temperature dependence of the reaction rate k (3), and after integration, Eq. (4) is obtained, which was used for fitting.

$$x(T) = \sqrt{\frac{2z}{\alpha} \int e^{-E/RT} dT} \tag{4}$$

The fit yielded an activation energy E = 80 kJ. Inserting the obtained values for z and E into Eq. (3), the Arrhenius plot yielded values which were in agreement with those in the literature [12].

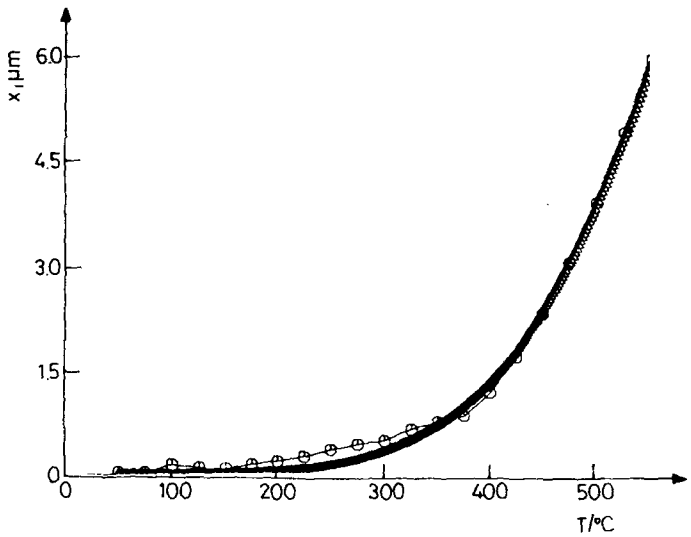

Fig. 5 Difference curve of a non-isothermal series measured with iron in air from 20°–550°C

The use of this approach is demonstrated by the detection of the Fe_3O_4 layer at temperatures where the formation of Fe_2O_3 is negligible and FeO is not yet formed. The procedure, however, can also be applied to series with more than one oxide layer obtained on heating beyond 570°C. In such a case the difference curves are formed only with the specific peaks of the different oxides. It should be noted that only when the X-rays penetrate the whole oxide layer are reasonable results obtained. For measurements of Fe_2O_3, which forms only thin layers, the application of grazing incidence is preferred [13, 14].

Further development of this procedure reported elsewhere [15] takes into account the absorption of the X-rays penetrating the oxide layers. This opens the possibility of determining the kinetics of several layers without the need of microscopic determination of the end thickness.

Conclusion

These examples show that TRXRD can successfully be used as a technique of thermal analysis. For phase transitions the participating phases can be identified, and in the case of solid-state reactions the difference procedure allows calculation of kinetic parameters from isothermal and non-isothermal experiments.

* * *

We are indebted to Mr. K. O. Hartmann, Ms. Juez Lorenzo and Mr. H. G. Farr for their assistance during the measurements and for the maintenance of the measuring systems.

References

1 N. Bett and A. M. Glazer, J. Phys. E., (1972) 1178.
2 A. M. Glazer, J. Appl. Cryst., 5 (1972) 420.
3 R. Clarke and R. E. Morley, J. Appl. Phys., 9 (1976) 481.
4 B. B. Giessen and G. E. Gordon, Science, 159 (1968) 973.
5 K. Heide, Z. Anorg. Chem., 344 (1966) 241.
6 W. Engel and N. Eisenreich, Thermochim. Acta, 83 (1985) 161.
7 A. Deimling, W. Engel and N. Eisenreich, J. Thermal Anal., 38 (1992) 843.
8 N. Eisenreich and W. Engel, J. Appl. Cryst., 16 (1983) 259.
9 A. N. Campbell and A. J. R. Campbell, Canad. J. Research, 24 B (1946) 93.
10 J. R. Holden and C. W. Dickinson, J. Phys. Chem., 79 (1975) 249.
11 N. Eisenreich and W. Engel, J. Thermal Anal., 35 (1989) 577.
12 V. Kolarik, M. Juez Lorenzo, N. Eisenreich and W. Engel, J. Thermal Anal., 38 (1992) 649.
13 M. F. Toney and T. C. Fuang, J. Mat. Res., 3 (1988) 351.
14 N. Eisenreich, W. Engel, V. Kolarik, M. Juez Lorenzo and A. Rehfeldt-Oskierski, Materials Science Forum, 79–82 (1991) 613.
15 V. Kolarik, N. Eisenreich and W. Engel, Proc. of the European Powder Diffraction Conference 2 (EPDIC2) in press.

Zusammenfassung — Anhand von Beispielen der Phasenumwandlung, Feststoffreaktionen und Hochtemperaturkorrosion wird die thermoanalytische Anwendung von TRXRD gezeigt. Das Meßsystem liefert eine Reihe von Diffraktionskurven, die mittels eines Differenzverfahrens ausgewertet wurden, welches Daten zu Kurven verarbeitet, die weiterhin mit DSC- und TG-Kurven vergleichbar sind und sich somit für eine kinetische Untersuchung eignen.